

Hydrogen Gas Sensor Based on Ultrasonicated Polyaniline and Tin Oxide Composite Nanofibers

Hemlata J. Sharma¹, Diptee V. Jamkar², Subhash B. Kondawar³

^{1,2,3}Department of Physics, R. T. M. Nagpur University, Nagpur – 440033, India

Abstract: Nanofibers of semiconducting metal-oxides have been widely utilized for applications in gas sensors due to highly surface reaction between the metal-oxides and adsorbed gas species but require the high operating temperature (200-400°C). The conducting polymers have improved many aspects of the gas sensors especially in lowering the operating temperature to around room temperature. In addition to this, the ability to incorporate specific binding sites into conducting polymer promises it for the improvement of selectivity and sensitivity of material. Therefore, in this paper we report the fabrication of ultrasonicated polyaniline (PANI) and tin oxide (SnO₂) composite nanofibers using electrospinning technique and characterization for hydrogen gas sensing application. In a typical procedure, ultrasonicated as-synthesized polyaniline (PANI) and SnCl₂·2H₂O in dimethyl formamide (DMF) solution was mixed with ethanol under vigorous stirring. Subsequently, a carrier polymer PVP was added to form viscous solution for loading into glass syringe to fabricate the nanofibers collected on conducting aluminum foil using electrospinning. Ultrasonication of PANI and SnCl₂·2H₂O in DMF provided energy for the chemical reaction to speed up dispersion of PANI in the solution. The as-prepared PANI/SnO₂ nanofibers were investigated for structural characterizations by means of FTIR, UV-VIS, SEM and XRD. The morphologically non-woven nanofibers with highly porous and agglomerated structure of diameter around 300-500 nm was confirmed by SEM image. FTIR and UV-VIS spectra revealed the possible incorporation of SnO₂ in PANI and confirmed the uniform attachment of PANI on the surface of SnO₂ nanostructures. XRD pattern showed the presence of tetragonal SnO₂ and the crystalline structure of SnO₂ was not affected with the incorporation of PANI. The as-prepared nanofibers of PANI/SnO₂ nanocomposite showed improved hydrogen sensing properties at very low temperature as compared to that of pristine SnO₂ nanofibers.

Keywords: Nanofibers; tin oxide; polyaniline; ultrasonication; electrospinning; hydrogen sensing;

1. Introduction

Nanofibers have attracted the attention of researchers due to their remarkable micro and nano structural characteristics, high surface area, small pore size, and the possibility of their producing three dimensional structures that enable the development of advanced materials with sophisticated applications. Nanofibers can be identified as fibers having diameters between tens and hundreds of nanometers. This nanoscale diameter of fibers can give an enormous surface area per unit mass [1, 2]. Nanofibers of semiconducting metal-oxides have been widely utilized for applications in gas sensors due to their gas sensing properties largely based on the surface reaction between the metal-oxides and adsorbed gas species by measuring changes in their physical properties on exposure to specific gas.

Among the metal oxide, pure tin oxide, SnO₂ is a remarkable n-type semiconductor material having wide band gap (~ 3.6 eV) and by making use of small quantity of dopant into its matrix, thin film of this material find use in several devices such as flat panel displays, transparent electrodes, photo sensors, photo catalysts, antistatic coatings, solar cells and gas sensors for the detection of H₂, NH₃ and NO₂ gases [3, 4]. But, the high temperature operation of these sensors makes the life time of the sensor shorter and thus requires more power for operation. In addition, the high operating temperature (200-400°C) of these sensors may be inadequate for measuring high gas concentrations due to the danger of explosions [5-10].

The conducting polymers have improved many aspects of the gas sensors especially in lowering the operating temperature to around room temperature. Among the various conducting polymers, Polyaniline (PANI) has been investigated as a potential material for gas sensing

applications, due to its controllable electrical conductivity, environmental stability and interesting redox properties associated with the chain nitrogen's. It is the unique type of conducting polymer in which the charge delocalization can, in principle, offer multiple active sites on its backbone for the adsorption and desorption of gas analyte [11]. Therefore, there has been increasing interest of the researchers for the preparation of nanocomposites based on PANI. So, hybridization of metal oxide and conducting polymer could improve the properties of pure metal oxides or conducting polymers gas sensor and the new synthesized material shows the synergistic effect of these two materials. The Nanofibers of polymeric materials have large aspect ratio, large surface area to volume ratio and large porosity, such materials are best for sensing of different gases due to larger absorptive capacity for gas analyte [12-13]. However, hydrogen is colorless, odorless, and extremely flammable gas with lower explosive limit of 4% in air [14]. Thus, to meet the requirements, there have been significant efforts to enhance the sensitivity of hydrogen sensors. To ensure the safety of hydrogen, efficient and safety hydrogen sensors are still demanded [15].

In this work, a high-efficiency hydrogen sensor based on SnO₂/PANI composite nanofibers has been demonstrated via electrospinning technique and calcination procedure.

2. Experimental

2.1. Materials

SnCl₂·2H₂O, Aniline monomer (distilled under reduced pressure), ammonium peroxydisulphate (APS) and Polyvinyl pyrrolidone (PVP, Mw=1,300,000) were purchased from Aldrich. All supplement chemicals were of AR grade and used as received.

2.2. Preparation of SnO₂/ PANI Composite nanofibers

In a typical procedure, 0.4 g of SnCl₂·2H₂O was dissolved in 0.4 g of ultrasonicated PANI/CSA prepared from chemical oxidative method. Then, 4.4 g of DMF and 4.4 g of ethanol were mixed in it under vigorous stirring for 30 min. Subsequently, 1.0 g PVP was added into the above solution under vigorous stirring for 45 min. The mixture was loaded into a glass syringe with a needle of 0.5 mm in diameter at the tip and was electrified using a high-voltage DC supply. Calcination (400°C in air for 5 h) was performed to remove the organic constituents of PVP and crystallize the SnO₂. Electrospinning apparatus consists of a syringe pump, DC high voltage source and rotating or stationary collector. The spinning solution was kept in a vertical syringe with a stainless steel needle having an orifice of 0.5mm. The needle was electrically connected to a positive high voltage. 17 kV was provided between the tip of the spinning nozzle and the collector at a distance of 20 cm and the solution flow rate was kept at 0.4mL/h was maintained using computer control programmer. Thus, the fibers were prepared successfully.

3.Results and discussion

The as-prepared nanofibers were subjected to various characterizations. A variety of laboratory techniques are used to determine structure and properties of the nanostructures of nanocomposites. Various physico-chemical and spectral techniques can be used to determine composition of nanofibers of nanocomposites. There are various analytic methods that are available for the characterization of materials such as Scanning electron microscopy (SEM, Carl Zeiss Model EVO-18), X-ray Diffraction technique (XRD, PANalytical diffractometer with Cu K α), UV-Visible spectroscopy (SHIMADZU Spectrophotometer, Model-UV-1800) and Fourier transform infrared spectroscopy (FTIR, Bruker Alpha Spectrophotometer), Hydrogen gas sensing (Keithley instruments Inc-Model 2000).

3.1 Scanning Electron Microscopy (SEM)

Fig. 1 shows the SEM image of SnO₂ /PANI nanofibers. This technique used to study the morphology, topology and composition of a material. The diameter of nanofibers is found to be less than 500 nm. During the thermal treatment, PVP was removed and SnCl₂·2H₂O was converted into SnO₂, resulting in a rough surface occurring. SnO₂/PANI shows porous structure which causes better sensing properties even at low operating temperature.

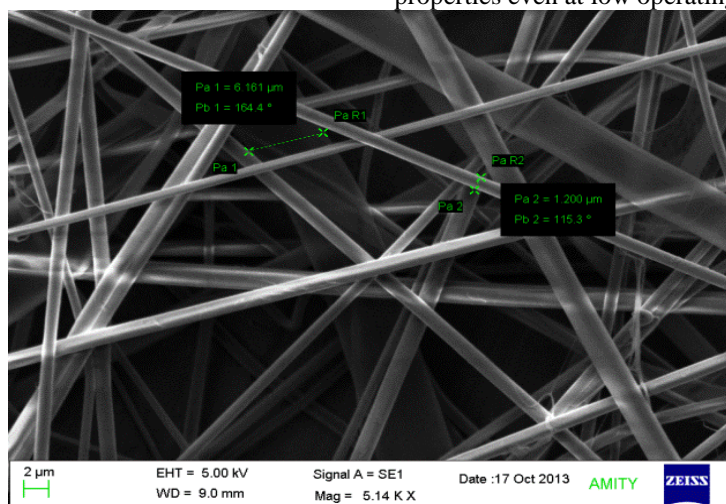


Figure 1: SEM image of SnO₂/PANI nanofibers

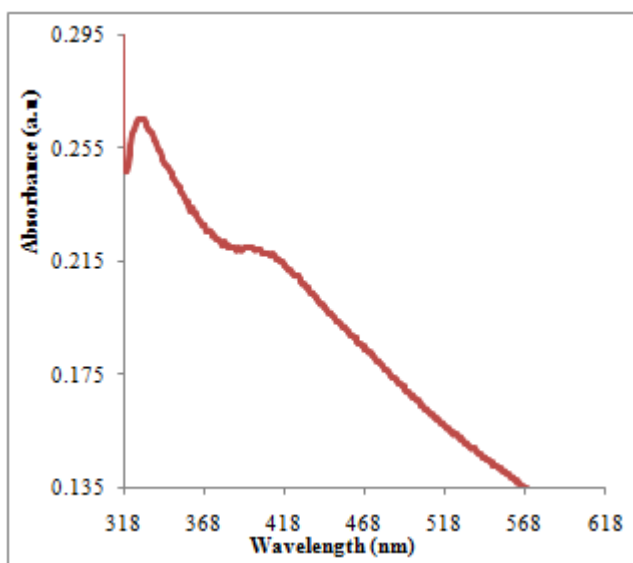


Figure 2: UV-VIS spectroscopy of SnO₂/PANI nanofibers

3.2 UV-VIS Spectroscopy

UV-VIS spectroscopy was utilized to understand the electronic states SnO₂/PANI. Fig. 2 shows UV-VIS spectra of SnO₂/PANI nanofibers. The SnO₂/PANI showed two characteristic bands, one at 407 nm in visible region corresponds to inter ring charge transfer ratio of benzenoid to quinoid moieties showing polaron- π^* transition and arises owing to the doping level and the formation of polarons [16-18] and other at 326 nm in UV corresponds to π - π^* transition of benzenoid ring and the insertion of SnO₂ in PANI.

3.3 Fourier Transform Infra-Red Spectroscopy (FTIR)

The FTIR spectra of SnO₂/PANI nanofibers are shown in Fig. 3, the peak at 3743 cm⁻¹ is associated with the interaction between SnO₂ and PANI by formation of hydrogen bonding between H-N and oxygen of SnO₂.The

vibration band seen around 2376 cm^{-1} and 2312 cm^{-1} has been ascribing to the aromatic C-H vibration.

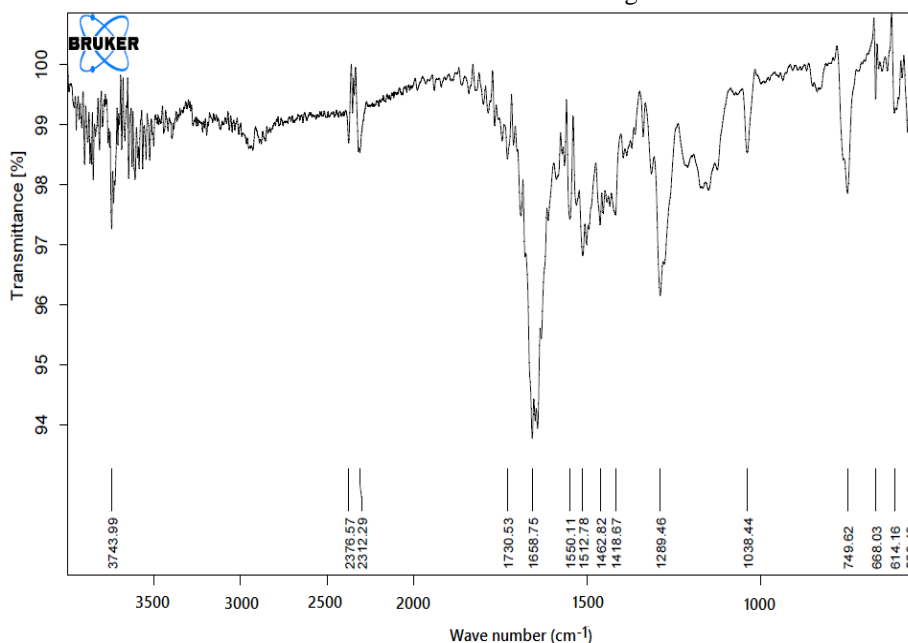


Figure 3: FTIR spectrum of SnO_2/PANI nanofibers

The $1550\text{-}1650\text{ cm}^{-1}$ vibration band is due to the C-N stretching vibration of quinoid rings whereas $1439\text{-}1498\text{ cm}^{-1}$ vibration band arises due to the C-N stretching vibration associated with the benzenoid ring. In the region close to 1350 cm^{-1} the peaks are attributed to the presence of aromatic amines present in polyaniline. The 1040 cm^{-1} vibration band is due to S=O bonding for camphor sulphonic acid and the peaks at around $650\text{-}750\text{ cm}^{-1}$ corresponds to the C-C, C-H bonding mode of aromatic ring and which is due to the Sn-O-Sn stretching.

3.3 X-Ray Diffraction Spectroscopy (XRD)

All the strong diffraction peaks of already reported pristine SnO_2 nanofibers can be perfectly indexed as the tetragonal rutile structure for SnO_2 (ICDD DATA CARD 41-1445) [19]. Fig. 4 shows the XRD patterns for SnO_2/PANI nanofibers. In the SnO_2/PANI nanofibers, most of the peaks are found to be broadened due the polycrystalline effect of PANI as compared to those of SnO_2 . The reduced intensity of the peaks was observed compared with the XRD of pure SnO_2 . The main dominant peaks of SnO_2 were identified at $2\theta = 26.66^\circ, 34.18^\circ, 52.3^\circ, 61.34^\circ, 64.4^\circ$ and 65.54° which corresponding to (1 1 0), (1 0 1), (2 1 1), (1 1 2), (3 0 1) and (3 0 2) and the three strong peaks are assigned to the (1 1 0), (1 0 1) and (2 1 1).

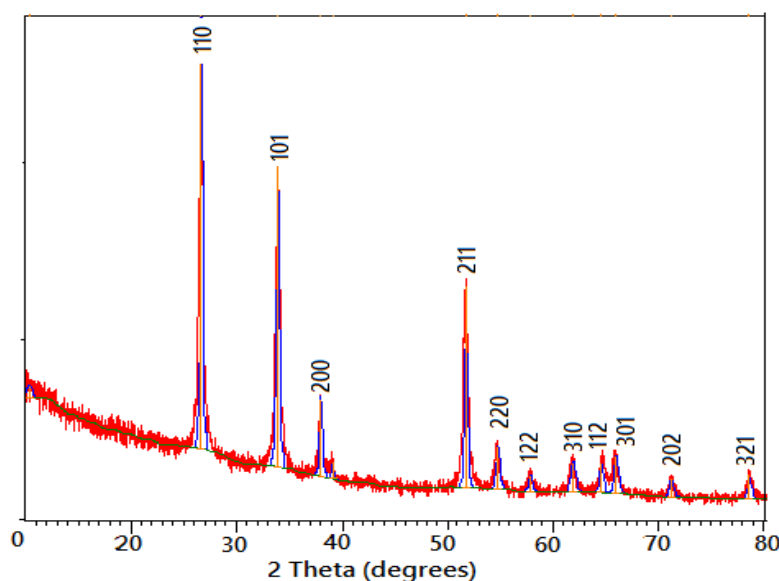


Figure 4: XRD pattern of SnO_2/PANI nanofibers

3.5 Hydrogen Gas Sensing

In order to systematically investigate the gas sensing properties of SnO_2/PANI nanocomposites sensors, the study

of gas sensing response with time and sensitivity with temperature was carried out towards 1000 of H_2 gas. Fig. 5 represents sensitivity to 1000 ppm of H_2 for the SnO_2/PANI composite nanofibers starting at room temperature with

increasing the temperature further. It was found that the SnO₂/PANI composite nanofibers sensor had better sensitivity and response to H₂ gas compared to the pristine SnO₂ as well as much lower operating temperature than the reported working temperature of pristine SnO₂ (about 200-400°C) [20]. As shown in Fig. 5, the sensitivity of the composite material increases and reaches its maximum at the temperature at 48°C.

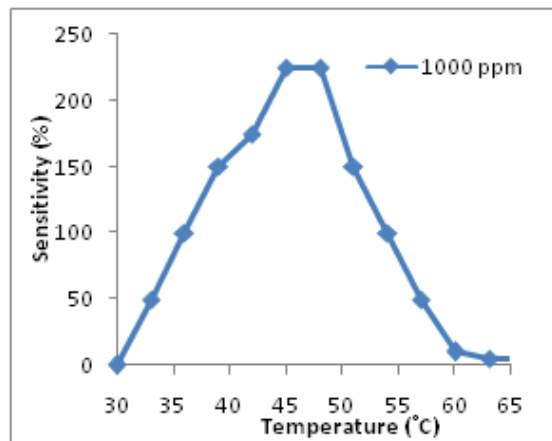


Figure 5: Sensitivity of 1000 ppm of SnO₂/PANI nanofibers

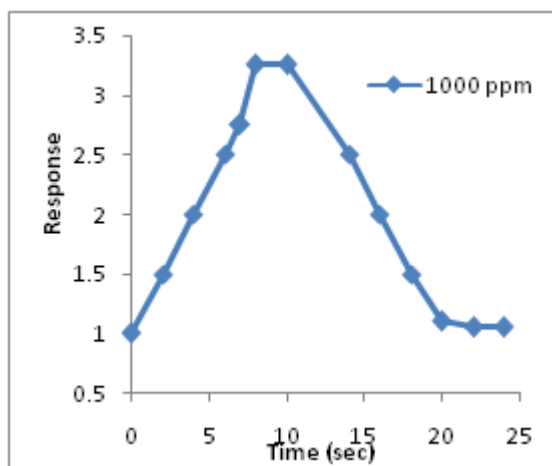


Figure 6: Response of H₂ for the SnO₂/PANI composite nanofibers at 1000 ppm

From literature survey, it is seen that there is no appreciable change noticed in the nanofibres film resistance for the case of pure tin oxide, on exposure to different concentrations of H₂ gas and tin oxide films remained insensitive to this gas at room temperature (RT). However, SnO₂/PANI nanocomposite films show appreciable sensitivity at 40°C and also we can see a large change in the film resistance on H₂ gas exposure. In the temperature range of 40-90°C, the maximum gas response is observed for SnO₂/PANI nanocomposite sensor around 48°C for both ppm.

On exposure to H₂ gas, the nanocomposite film resistance decreases by more than an order of magnitude from its original value, indicating that the electrical resistance of SnO₂/PANI composite films is a sensitive parameter in the presence of hydrogen gas. The response of sensor was monitored in terms of the normalized resistance calculated by $\text{Response} = R_0/R_g$ and the sensitivity factor was monitored in terms of the % sensitivity calculated by % sensitivity = $\Delta R/R_0$. Where ΔR is the variation in resistance

of composite films from baseline after exposure to H₂ gas, R_g is the resistance of the sensor in presence of H₂ gas and R₀ is the initial baseline resistance of the films.

The observed increased response in Fig. 6 on increasing the concentration of H₂ gas may be due to the creation of a positively charged depletion layer on the surface of SnO₂ nanofibers, which promotes the inter-particle electron transition between PANI and SnO₂ at the heterojunction; this would cause a reduction of activation energy and enthalpy of physisorption for H₂ gas. As per the definitions of 'Response time (R_p)' and 'Recovery time (R_c)' for gas sensing, the values of R_p and R_c were estimated to be ~3 sec and ~4 sec respectively. Over a long period of hydrogen exposure it was observed that SnO₂/PANI composite film sensor exhibited a good stability and repeatability as gas sensor with consistent pattern and response when exposed to the H₂ gas close to room temperature.

4. Conclusion

The nanofibers of SnO₂/PANI composite were synthesized successfully for H₂ sensing via electrospinning technique. SEM revealed the fibers of SnO₂/PANI composite are in nanoregime. XRD proved to be crucial to analyze the structural and morphological properties of nanocomposite films so as to improve their characteristics and subsequently for the development of gas sensor. Optical absorbance studies show the characteristic peaks for SnO₂/PANI. FTIR study shows presence of the Sn-O-Sn vibrational peak and characteristic vibrational peaks of PANI indicating the interaction of SnO₂ particles in PANI matrix. The SnO₂/PANI hybrid material showed sensitivity to H₂ gas at room temperature and when operated at 48°C, nanocomposite films exhibited maximum sensitivity. The proposed sensing mechanism was related to the existence of p-n heterojunction in the SnO₂/PANI hybrid material. It is observed that in comparison to the pure SnO₂ and PANI based sensors reported earlier, the SnO₂/PANI sensor in the present study exhibits the faster response and higher sensitivity for hydrogen gas.

5. Acknowledgement

The authors acknowledge Department of Science & Technology, New Delhi (India) for financial assistance under; INSPIRE Fellowship 2013. Sanction Order No. & Date: DST/INSPIRE Fellowship/2013/92, dated 17th May 2013. Registration No: [IF130149].

References

- [1] W. Zhang, C. Wang, T. C. Wen, Y. Wei, Progress in Polymer Science 36 (2011) 671–712.
- [2] Y. Z. Long, M. M. Li, C. Gu, M. Wan, J. L. Duvail, Z. Liu, Z. Fan, Progress in Polymer Science 36 (2011) 1415-1442.
- [3] H. Tai, Y. Jiang, G. Xie, J. Yu, X. Chen, Sensors and Actuators B 125 (2007) 644–650.
- [4] J. Qiu, S. Zhang, H. Zhao, Sensors and Actuators B 160 (2011) 875–890.
- [5] N.V. Hieu, H.R. Kim, B.K. Ju, J.H. Lee, Sens. Actuators B: Chem. 133 (2008) 228–234.

- [6] J. Hu, Y. Bando, Q. Liu, D. Golberg, Adv. Funct. Mater. 13 (2003) 493–496.
- [7] Q. Kuang, C. Lao, Z.L. Wang, Z. Xie, L. Zheng, J. Am. Chem. Soc. 129 (2007) 6070–6071.
- [8] X.Y. Xue, Y.J. Chen, Y.G. Wang, T.H. Wang, Appl. Phys. Lett. 86 (2005) 233101/1–1233101/.
- [9] Y. Zhang, X. He, J. Li, Z. Miao, F. Huang, Sens. Actuators B: Chem. 132 (2008) 67–73.
- [10] A. Kolmakov, D.O. Klenov, Y. Lilach, S. Stemmer, M. Moskovits, Nano Lett. 5 (2005) 667–673.
- [11] S.R. Kargirwar, S.R. Thakare, M.D. Choudhary, S.B. Kondawar, S.R. Dhakate, Advanced Materials Letters 2 (2011) 397-401.
- [12] S. Matsushima, T. Maekawa, J. Tamaki, N. Miura, N. Yamazoe, New Sensors and Actuators B 9 (1992) 71-78.
- [13] Y. Fong, J.B. Schlenoff, Polymer 36 (1995) 639-643.
- [14] C.W. Hung, H.L. Lin, H.I. Chen, Y.Y. Tsai, P.H. Lai, S.I. Fu, H.M. Chuang, W.C. Liu, Sensors and Actuators B: Chemical 122 (2007) 81-88.
- [15] A. Kolmakov, M. Moskovits, Annual Review of Materials Research 34 (2004) 151-180.
- [16] A.G. MacDiarmid, A.J. Epstein, Synthetic Metals 65 (1994) 103-116.
- [17] H. Jiang, Y. Geng, J. Li, F. Wang, Synthetic Metals 84 (1997) 125-126.
- [18] B.J. Kim, S.G. Oh, M.G. Han, S.S. Im, Synthetic Metals 122 (2001) 297-304.
- [19] S.J. Chang, T.J. Hsueh, I.C. Chen, S.F. Hsieh, S.P. Chang, C.L. Hsu, Y.R. Lin, B.R. Huang, IEEE Transactions on Nanotechnology 7 (2008) 754-759.
- [20] X. Xu, J. Sun, H. Zhang, Z. Wang, B. Dong, T. Jiang, W. Wang, Z. Li, C. Wang, Sensors and Actuators B 160 (2011) 858–863.